

## A NOVEL LPI METHOD OF RADAR'S ENERGY CONTROL

Z. K. Zhang<sup>1, 2, \*</sup> and J. J. Zhou<sup>1</sup>

<sup>1</sup>College of Electronic and Information Engineering, Nanjing University of Aeronautics and Astronautics, Nanjing 210016, China

<sup>2</sup>College of Electronic Information, Jiangsu University of Science and Technology, Zhenjiang 212003, China

**Abstract**—A novel radar energy control strategy based on an improved Interacting Multiple Model Particle Filter (IMMPF) tracking method is presented in this paper. Firstly, the IMMPF tracking method is improved by increasing the weight of the particle which is close to the system state and updating the model probability of every particle. Based on this improved IMMPF method, an energy control method for Low Probability of Intercept (LPI) is then presented, which controls the emission time and power of radar according to the target's range and radar cross section (RCS), under the condition of constant detection probability. The tracking accuracy and LPI performance are demonstrated in the Monte Carlo simulations. The results are validated through the comparisons with other methods.

### 1. INTRODUCTION

In order to achieve important tactical requirement of LPI, dynamically controlling the emission of a radar during sensor management is very necessary. As we know, less radar emission means more excellent performance of the LPI. An LPI management algorithm for multiple sensors is proposed in [1], by formulating the problem as a partially observed Markov decision process (POMDP) with an on-going multi-armed bandit structure. A circular equivalent vulnerable radius [2], as a function of three sets of parameters — the interceptor performance, emitter antenna pattern, and geometric/link parameters, is used to quantify the LPI capability of a waveform. Many LPI waveforms [3, 4]

---

*Received 3 August 2012, Accepted 26 September 2012, Scheduled 1 October 2012*

\* Corresponding author: Zhen Kai Zhang (zzk@nuaa.edu.cn).

have also been designed to minimize the probability of intercept by an enemy receiver. LPI performance factor is derived and applied in [5]. The work in [6] analyses the effect of the LPI strategies and considers whether there are any fundamental limits to the ability to detect radar emissions. Those works only concern the problem of LPI ability for the radar. However, the radar should have not only good LPI capability, but also excellent detection and tracking performance.

Target tracking is one of the critical problems in the airborne surveillance systems. As we know, for targets with fixed kinematic behavior, a single model state estimator is sufficient for tracking targets. However, for targets with varying or multiple kinematic behaviors, the interacting multiple model (IMM) [7–9] is often employed. The IMM estimator is widely accepted as one of the most cost-effective dynamic multiple model methods and has been shown to achieve high performance with relatively low complexity.

The models of the target dynamics and the observations often exhibit nonlinearities; the filtering should take into account of or at least be robust against these characteristics. Particle filters [10–12] have been introduced to deal with these nonlinearities in the dynamics and measurements. Particle filter is based on Bayesian estimation theory which gives an optimal solution [13] when the dynamic behavior of the object is uncertain and the measurement of the object nondeterministic. As the maneuvering target tracking could be formulated as a multiple model nonlinear filtering problem [14], a new method combing the interacting multiple model approach with a particle filter approach is presented in [15], which is able to deal with nonlinearities and non-Gaussian noise in a mode.

In this paper, we improve the IMMPPF algorithm in [15] for more accurate estimates for tracking targets. We first use the similarity between the particles and the system state to modify the weight of the particle. And the estimate of the state is obtained by computing the mode probability of every particle. Based on the improved IMMPPF algorithm, a novel algorithm of energy control for LPI is proposed. Under the condition of constant detection probability, the radar's energy is adaptively designed according to different ranges and RCSs of the target.

The remainder of this paper is organized as follows. Sections 2 and 3 describe the improved IMMPPF algorithm of target tracking and the energy control methods for LPI in details, respectively. Simulations of the proposed algorithms and comparison results with other methods are provided in Section 4. The conclusions are presented in Section 5.

## 2. IMPROVED IMMPF ALGORITHM OF TARGET TRACKING

The IMMPF tracking method is improved by increasing the weight of the particle which is close to the system state and updating the model probability of every particle in Sections 2.4 and 2.5, respectively.

### 2.1. System Setup

Given the system at time  $k$

$$\mathbf{X}_k = \mathbf{F}\mathbf{X}_{k-1} + \mathbf{U}_{k-1} \quad (1)$$

$$\mathbf{Z}_k = \mathbf{H}(\mathbf{X}_k) + \mathbf{V}_k \quad (2)$$

where,  $\mathbf{X}_k = [x_k, \dot{x}_k, y_k, \dot{y}_k]$  is the dynamical state of the system, and  $(x_k, \dot{x}_k)$  and  $(y_k, \dot{y}_k)$  are respectively the range, velocity of the direction of  $X$  and  $Y$ .  $\mathbf{U}_{k-1}$  and  $\mathbf{V}_k$  are the process noise matrix and measurement noise matrix.  $\mathbf{F}$  is the dynamic matrix of the system and  $\mathbf{Z}_k$  the measurement vector. As we know, the signal to noise ratio of the measurement vector is decided by the emitted energy. Radar is a typical active sensor which provides both range and angle measurements for target tracking. For concise description, the elevation angle is supposed to be zero here. The measurement vector of the radar is composed of  $\mathbf{Z}_{rRk}$  and  $\mathbf{Z}_{\theta Rk}$  which are the measurement of the range  $r$  and azimuth angle  $\theta$ .

$$\mathbf{Z}_{rRk} = \sqrt{x_k^2 + y_k^2} + \mathbf{V}_{rRk} \quad (3)$$

$$\mathbf{Z}_{\theta Rk} = \arctan \frac{y_k}{x_k} + \mathbf{V}_{\theta Rk} \quad (4)$$

where  $(\mathbf{Z}_{rRk})^2/(\mathbf{V}_{rRk})^2 = S_{NR}^k$  and  $(\mathbf{Z}_{\theta Rk})^2/(\mathbf{V}_{\theta Rk})^2 = S_{NR}^k$ .  $S_{NR}^k$  is the signal to noise ratio of the radar's echo at time  $k$ , which is decided by the emitted energy. It also has an impact on the tracking accuracy.

There are  $M$  kinematics models and  $N$  particles for every model in the system.

### 2.2. Interaction

Compute mixing probabilities:

$$\boldsymbol{\mu}_{k-1}^l(m_k|m_{k-1}) = \frac{p_{ij}\boldsymbol{\mu}_{k-1}^l(m_{k-1})}{\mathbf{b}_{k-1}^l(m_k)} \quad (5)$$

where the model  $m_k$  is set at time  $k$ .  $p_{ij}$  is the Markov transition probability from model  $m_{k-1}$  to model  $m_k$  and  $\boldsymbol{\mu}_k^l(m_k)$  the mixing

probability of the  $l$ th particle for model  $m_k$ ,  $l = 1, 2, \dots, N$ .  $\mathbf{b}_{k-1}^l(m_k)$  is the normalizing factor:

$$\mathbf{b}_{k-1}^l(m_k) = \sum_{m_{k-1} \in M} p_{ij} \boldsymbol{\mu}_{k-1}^l(m_{k-1}) \quad (6)$$

$\bar{\mathbf{x}}_{k-1}^l(m_k)$  is obtained by the interaction with the other models:

$$\begin{aligned} & \bar{\mathbf{x}}_{k-1}^l(m_k) \\ = & \sum_{m_{k-1} \neq m_k}^M \left[ \hat{\mathbf{x}}_{k-1}^l(m_{k-1}) \boldsymbol{\mu}_{k-1}^l(m_{k-1} | m_k) + \hat{\mathbf{x}}_{k-1}^l(m_k) \boldsymbol{\mu}_{k-1}^l(m_k | m_k) \right] \quad (7) \end{aligned}$$

### 2.3. Prediction Stage

Predicted sample of every particle at time  $k$ :

$$\bar{\mathbf{x}}_k^l(m_k) = \mathbf{F}(m_k) \bar{\mathbf{x}}_{k-1}^l(m_k) + \mathbf{u}_{k-1}^l(m_k) \quad (8)$$

Predicted output:

$$\bar{\mathbf{z}}_k^l(m_k) = \mathbf{H} \left( \bar{\mathbf{x}}_k^l, m_k \right) \quad (9)$$

### 2.4. Modification of the Weight for the Particle

If the measurement vector of a particle is close to the measurement vector of the true state, its vector will be close to the vector of the true state. So it is helpful to increase the influence of those particles which are closer to the true state, for obtaining more accurate tracking results.

$\bar{\mathbf{z}}_k^l(m_k)$  is the estimation of azimuth angle  $\bar{\boldsymbol{\theta}}_R^l(m_k)$  and range  $\bar{\mathbf{r}}_R^l(m_k)$  from the  $l$ th particle at time  $k$ .  $\mathbf{PCC}_{\theta_R, k}^l(m_k)$  and  $\mathbf{PCC}_{r_R, k}^l(m_k)$  are respectively the Pearson correlation coefficient of the azimuth angle and range, which are used to measure the similarity of the two vectors.

$$\begin{aligned} & \mathbf{PCC}_{\theta_R, k}^l(m_k) \\ = & \frac{\sum_{i=k-P+1}^k \left( \bar{\boldsymbol{\theta}}_R^l(m_i) - (\bar{\boldsymbol{\theta}}_R^l(m_i))^* \right) (\mathbf{Z}_{\theta_R i} - (\mathbf{Z}_{\theta_R i})^*)}{\sqrt{\sum_{i=k-P+1}^k \left( \bar{\boldsymbol{\theta}}_R^l(m_i) - (\bar{\boldsymbol{\theta}}_R^l(m_i))^* \right)^2 \sum_{i=k-P+1}^k \left( \mathbf{Z}_{\theta_R i} - (\mathbf{Z}_{\theta_R i})^* \right)^2}} \quad (10) \end{aligned}$$

$$\begin{aligned} & \mathbf{PCC}_{r_R,k}^l(m_k) \\ = & \frac{\sum_{i=k-P+1}^k (\bar{\mathbf{r}}_R^l(m_i) - \bar{\mathbf{r}}_R^l(m_i)^*) (\mathbf{Z}_{r_R i} - (\mathbf{Z}_{r_R i})^*)}{\sqrt{\sum_{i=k-P+1}^k (\bar{\mathbf{r}}_R^l(m_i) - \bar{\mathbf{r}}_R^l(m_i)^*)^2 \sum_{i=k-P+1}^k (\mathbf{Z}_{r_R i} - (\mathbf{Z}_{r_R i})^*)^2}} \end{aligned} \quad (11)$$

where  $(\cdot)^*$  means the average value of the past  $P$  numbers.

Then  $\mathbf{PCC}^l(m_k)$  is given by:

$$\mathbf{PCC}^l(m_k) = \frac{1}{2} \left( \mathbf{PCC}_{\theta_R,k}^l(m_k) + \mathbf{PCC}_{r_R,k}^l(m_k) \right) \quad (12)$$

The weight update equation can be given by:

$$\bar{\mathbf{w}}_k^l(m_k) = \mathbf{PCC}^l(m_k) \mathbf{p}_{v_k(m_k)} \left( \mathbf{z}_k - \bar{\mathbf{z}}_k^l(m_k), 0 \right) \quad (13)$$

where  $\mathbf{p}_{v_k(m_k)}(\cdot)$  is the probability density of the measurement noise  $\mathbf{v}_k(m_k)$ .

The normalized weight can be given:

$$\bar{\mathbf{w}}_k^l(m_k) = \bar{\mathbf{w}}_k^l(m_k) / \sum_{l=1}^N \bar{\mathbf{w}}_k^l(m_k) \quad (14)$$

The new weight after the importance sampling is set as follows:

$$\bar{\mathbf{w}}_k^l(m_k) = 1/N \quad (15)$$

### 2.5. Update of the Model Probability

The common methods often update the model probability by the average residual matrix of all the particles and ignore the model character of single particle. Therefore, the model probability of every particle is updated here.

Residual covariance matrix of the  $l$ th particle is obtained as:

$$\mathbf{S}_k^l(m_k) = \mathbf{r}_k^l(m_k) \mathbf{r}_k^l(m_k)^T \quad (16)$$

where  $\mathbf{r}_k^l(m_k)$  represents the residual vector and can be given by:

$$\mathbf{r}_k^l(m_k) = \mathbf{z}_k - \mathbf{H} \left( \bar{\mathbf{x}}_k^l, m_k \right) \quad (17)$$

The likelihood function of the model is:

$$\Lambda_k^l(m_k) = \sqrt{|2\pi \mathbf{S}_k^l(m_k)|} \exp \left( -\frac{1}{2} \left( \mathbf{r}_k^l(m_k) \right)^T \left( \mathbf{S}_k^l(m_k) \right)^{-1} \mathbf{r}_k^l(m_k) \right) \quad (18)$$

The updated model probability can be given by:

$$\boldsymbol{\mu}_k^l(m_k) = \frac{\boldsymbol{\Lambda}_k^l(m_k)\mathbf{b}_{k-1}^l(m_k)}{B_k^l} \quad (19)$$

where  $B_k^l = \sum_{m_k \in M} \boldsymbol{\Lambda}_k^l(m_k)\mathbf{b}_{k-1}^l(m_k)$ .

## 2.6. Combination Stage

The estimate of the state is obtained as:

$$\hat{\mathbf{x}}_k^{\bar{=}} = \sum_{m_k=1}^M \sum_{l=1}^N \bar{\mathbf{w}}_k^l \bar{\mathbf{x}}_k^l(m_k) \boldsymbol{\mu}_k^l(m_k) \quad (20)$$

## 3. STRATEGY OF ENERGY CONTROL

Phased array radars [16] have the capability to switch the direction of the radar beam very quickly without inertia. So it is very free to decide the beam position and emitted energy to update the established track. The energy control methods for LPI of the phased array radar are proposed in this section.

### 3.1. Intercept Probability

The intercept probability [17]  $P_I$  is defined as

$$P_I = MF(2P_R/P_{SI})^{C_0} D_I T_{OT}/T_I \quad (21)$$

where  $MF$  is the mainlobe footprint (3 dB),  $P_{SI}$  the required power at intercept receiver for detection,  $D_I$  the density of intercept receivers per  $\text{km}^2$ , and  $C_0$  the sensitivity scaling factor. These parameters in the later simulation are drawn from [17]. Table 1 shows the parameters' values.

$T_{OT}$  and  $T_I$  denote the illumination time by emitter and the interceptor search time, respectively.  $T_I$  is assumed to be the total tracking time.  $P_R$  is the received power at intercept receiver, which can be defined as

$$P_R = \frac{P_T G_{TI} G_I \lambda^2 G_{IP} L_I}{(4\pi)^2 R_I^2} \quad (22)$$

**Table 1.** Values of the parameters.

Parameter	$MF$	$P_{SI}$	$C_0$	$D_I$
Value	11.2	$5 \times 10^{-12}$	0.477	0.001

where  $P_T$  is the emitted power of the radar,  $G_{TI}$  the antenna gain of the radar in the direction of the intercept receiver,  $G_I$  the antenna gain of the intercept receiver,  $G_{IP}$  the processing gain of the intercept receiver,  $R_I$  the interception range,  $\lambda$  the wavelength, and  $L_I$  the interceptor system loss.

As we know, it is difficult to design  $MF$ ,  $P_{SI}$ ,  $D_I$  and  $T_I$  as they are decided by the performance of the interceptor instead of the radar, so we have to reduce the radar's emission time  $T_{OT}$  or power  $P_T$  to lower the probability of intercept of the radar system. According to [17],  $P_R$  is equal to  $P_T \times 9.003 \times 10^{-9}$  here.

During the tracking process, the cumulative probability of intercept  $P_{Icum}$  is defined as:

$$P_{Icum} = 1 - \prod_{i=1}^I (1 - P_I^i) \quad (23)$$

$P_I^i$  is the  $i$ th intercept probability and  $I$  the intercept times.

### 3.2. Design of Emission Energy

Radar equation at time  $k$  is as follows:

$$R_k^4 = t_B^k \frac{P_{av}^k G_T G_R \lambda^2 \sigma_k}{(4\pi)^3 K T_R S_{NR}^k L} \quad (24)$$

where  $t_B^k$  is the single dwelling time of the beam from the normal direction at time  $k$ ,  $P_{av}^k$  the average radiated power,  $G_R$  the receiver gain,  $\sigma_k$  the radar cross section (RCS) of the target,  $K$  Boltzmann constant,  $T_R$  and  $L$  respectively effective noise temperature and radar system loss,  $R_k$  the detection range,  $G_T$  the transmit gain, and  $S_{NR}^k$  the signal to noise ratio of the radar's echo at time  $k$ . Detection probability [18]  $P_d^k$  at time  $k$  can be given as:

$$P_d^k = p_{fa}^{1/(1+S_{NR}^k)} \quad (25)$$

where  $p_{fa}$  is the false alarm probability of the radar.

Suppose that when the target whose range and RCS are respectively  $R_{max}$  and  $\sigma_{min}$ , the radar has to emit the maximum power  $P_{av max}$  with maximum dwelling time  $t_{B max}$ . Radar equation and the detection probability respectively become:

$$R_{max}^4 = t_{B max} \frac{P_{av max} G_T G_R \lambda^2 \sigma_{min}}{(4\pi)^3 K T_R S_{NR max} L} \quad (26)$$

$$P_d = p_{fa}^{1/(1+S_{NR max})} \quad (27)$$

The detection probability is supposed to meet the requirement of constant  $P_d$  during the whole tracking process. So  $S_{NR}^k$  at time  $k$  should be equal to  $S_{NR\max}$ . Combining (24) with (26), the emitting energy at time  $k$  can be written as:

$$P_{av}^k t_B^k = \frac{P_{av\max} t_{B\max} \sigma_{\min}}{R_{\max}^4} \frac{R_k^4}{\sigma_k} \quad (28)$$

However, during the tracking process,  $R_k$  and  $\sigma_k$  are unknown before radar detection.  $R_k$  is replaced by  $R_k^{pre}$  which is predicted by  $R_{k-1}$  and  $v_{k-1}$ .  $R_k^{pre}$  is presented as

$$R_k^{pre} = R_{k-1} + v_{k-1}T \quad (29)$$

where  $R_{k-1}$  and  $v_{k-1}$  are the target's range and velocity estimated by the tracking algorithm at time  $k-1$ , and  $T$  is the tracking interval.

As we know, RCS is the ratio of the scattered power to the incident power in the direction of an observer at infinity [17] and can be computed by the fundamental RCS equation once the radar echo is received. The RCS  $\sigma_{k-1}$  at time  $k-1$  is supposed to be known here. It is difficult to predict a target's RCS, so  $\sigma_k$  is replaced by  $\sigma_{k-1}$ .

So (28) becomes

$$P_{av}^k t_B^k = \frac{P_{av\max} t_{B\max} \sigma_{\min}}{R_{\max}^4} \frac{(R_k^{pre})^4}{\sigma_{k-1}} \quad (30)$$

In addition, the emitted energy methods of adaptive power (I-IMMPF-A-P) and adaptive time (I-IMMPF-A-T) are presented based on the improved IMMPF algorithm.

**I-IMMPF-A-P:**  $t_B^k = t_{B\max}$ , and  $P_{av}^k$  is designed according to change of the target range and target RCS.

$$P_{av}^k = \frac{P_{av\max} \sigma_{\min}}{R_{\max}^4} \frac{(R_k^{pre})^4}{\sigma_{k-1}} \quad (31)$$

**I-IMMPF-A-T:**  $P_{av}^k = P_{av\max}$ , and  $t_B^k$  is designed according to change of the target range and target RCS too.

$$t_B^k = \frac{t_{B\max} \sigma_{\min}}{R_{\max}^4} \frac{(R_k^{pre})^4}{\sigma_{k-1}} \quad (32)$$

After the emission time and power are designed, the radar equation can be given:

$$S_{NR}^k = t_B^k \frac{P_{av}^k G_T G_R \lambda^2 \sigma_k}{(4\pi)^3 K T_R L R_k^4} \quad (33)$$

Combined with (26),  $S_{NR}^k$  can be written as:

$$S_{NR}^k = \frac{P_{av}^k}{P_{av \max}} \frac{t_B^k}{t_{B \max}} \frac{R_{\max}^4}{R_k^4} \frac{\sigma_k}{\sigma_{\min}} S_{NR \max} \quad (34)$$

We can see that the emitted energy and signal to noise ratio influence each other during the tracking process.

#### 4. SIMULATION RESULTS

In this section, Monte Carlo simulations are performed to analyze the performance of the improved IMM PF and the proposed energy control method. The IMM filter here is composed of Constant Velocity model (CV)  $F_{CV}$  and Coordinated Turn rate model (CT)  $F_{CT}$ .

$$F_{CV} = \begin{bmatrix} 1 & T & 0 & 0 \\ 0 & 1 & 0 & 0 \\ 0 & 0 & 1 & T \\ 0 & 0 & 0 & 1 \end{bmatrix} \quad (35)$$

$$F_{CT} = \begin{bmatrix} 1 & \frac{\sin \omega T}{\omega} & 0 & \frac{1 - \cos \omega T}{\omega} \\ 0 & \cos \omega T & 0 & \frac{\sin \omega T}{\omega} \\ 0 & \frac{1 - \cos \omega T}{\omega} & 1 & \frac{\sin \omega T}{\omega} \\ 0 & \sin(\omega T) & 0 & \cos \omega T \end{bmatrix} \quad (36)$$

where  $T$  is the sampling interval,  $\omega$  the turn factor,  $T = 1$  s, and  $\omega = 0.1$ . In the simulation,  $M_c$  is the number of the Monte-Carlo simulation,  $K$  the total tracking time in every simulation,  $M_c = 500$ , and  $K = 100$ .

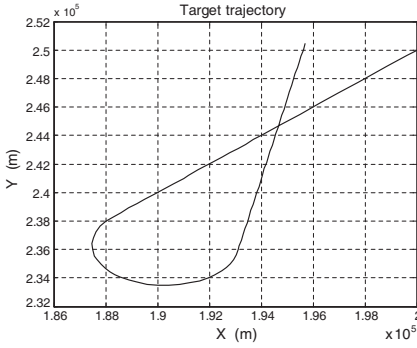
##### 4.1. Trajectory Design

Table 2 is the description of the trajectory in detail.

Figure 1 shows the target trajectory in 100s. The RCS of the target is designed in Fig. 2.

**Table 2.** Model description of the trajectory.

Time (s)	2–20	41–65	66–100
Target model	CV	CT	CV



**Figure 1.** Trajectory of the target.

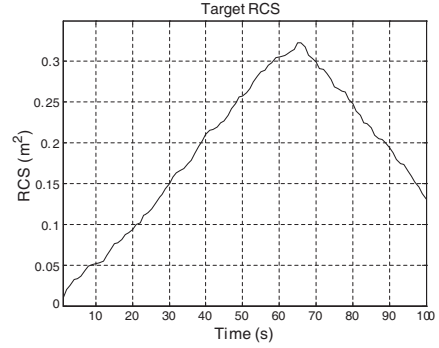


**Figure 2.** RCS of the target.

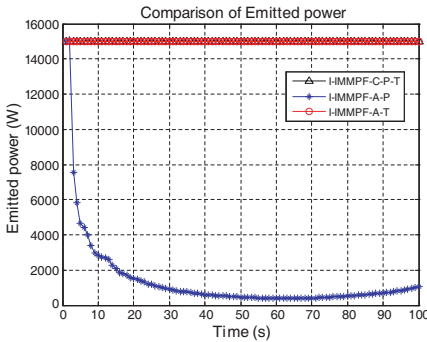


**Figure 3.** Comparison of Emitted power.

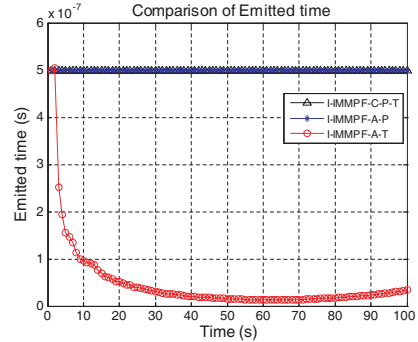


**Figure 4.** Comparison of Emitted time.

## 4.2. Comparison of LPI Performance

Based on the proposed improved IMMPF algorithm, the emitted energy methods of constant power and time (I-IMMPF-C-P-T), I-IMMPF-A-P and I-IMMPF-A-T are realized in the simulation. The three methods are described in Table 3. Emitted power of I-IMMPF-A-P and emission time of I-IMMPF-A-T are designed adaptively according to (31) and (32), respectively, which are also shown in Figs. 3 and 4.

Intercept probability is used to evaluate the LPI performance of the three methods. Fig. 5 illustrates their LPI performance. We can see that the I-IMMPF-A-T method has the best LPI ability as the emission time plays a more important role in the intercept probability computation. So the reduction of emission time is more effective.

**Table 3.** Energy control of the 3 methods.

Method	$P_{av}^k$ (W)	$t_B^k$ (s)
I-IMMPF-C-P-T	15000	$0.5 * 10^{-6}$
I-IMMPF-A-P	Adaptive	$0.5 * 10^{-6}$
I-IMMPF-A-T	15000	Adaptive

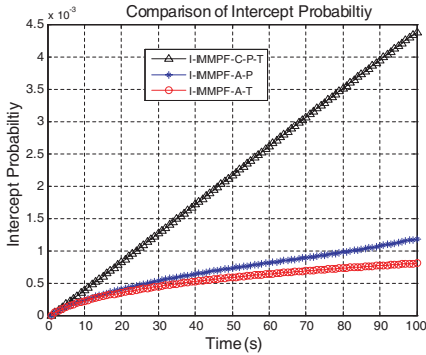


**Figure 5.** Comparison of intercept probability.

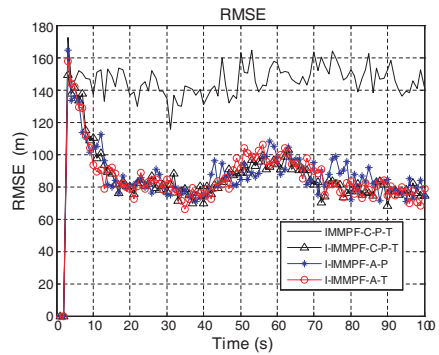


**Figure 6.** Comparison of RMSE.

### 4.3. Comparison of Tracking Performance

The root-mean-square error (RMSE) of time  $k$  and the average root-mean-square error (ARMSE) of the whole tracking process can be formulated as (37) and (38), respectively:

$$RMSE(k) = \sqrt{\frac{1}{M_c} \sum_{m=1}^{M_c} (x_k - \hat{x}_k^m)^2} \tag{37}$$

$$ARMSE = \frac{1}{K} \sum_{k=1}^K RMSE(k) \tag{38}$$

where  $x_k$  is the true state of the system and  $\hat{x}_k^m$  the estimated vector at the  $m$ th simulation.

The standard IMMPF method [15] with constant power and time (IMMPF-C-P-T) is also realized to compare the tracking accuracy with the improved one. RMSE and ARMSE of all methods with 250 particles are shown in Fig. 6 and Table 4, respectively, which show that the improved IMMPF method is more accurate than the standard IMMPF. However, the improved IMMPF method will spend

**Table 4.** Comparison of ARMSE.

Method	ARMSE (m)
IMMPF-C-P-T	142
I-IMMPF-C-P-T	85.0
I-IMMPF-A-P	86.6
I-IMMPF-A-T	85.5

a little more time on the computation, as it has to compute the Pearson correlation coefficient to modify the weight of the particles.

Comparing with I-IMMPF-C-P-T, we can see that the proposed method I-IMMPF-A-T and I-IMMPF-A-P not only reduce more emitted energy, but also present almost the same excellent tracking accuracy. Obviously, I-IMMPF-A-T has the best LPI ability with better tracking performance.

#### 4.4. Simulation Analysis

The improved IMMPF method achieves better tracking performance in the simulation, because it increases the weight of the particle which is close to the system state and updates the model probability of every particle. In addition, it involves the filtering for the current state and smoothing for the previous state.

Moreover, the proposed two energy control methods are more efficient than the common method which always emits constant power and time, because both the target's range and RCS are used to adaptively design the emitted time and power here. The LPI method depends on tracking algorithm as the target range has to be predicted every time.

## 5. CONCLUSIONS

In this paper, we have presented a new strategy of energy control for LPI based on an improved IMMPF approach. This method employs both the target's range and RCS to design the radar emitted energy with excellent tracking accuracy.

## ACKNOWLEDGMENT

This work was supported by The National Natural Science Foundation of China (61001150) and The Research and Innovation Foundation for Graduate Students in Jiangsu Province (CX10B\_110Z).

## REFERENCES

1. Krishnamurthy, V., "Emission management for low probability intercept sensors in network centric warfare," *IEEE Transactions on Aerospace and Electronics Systems*, Vol. 41, No. 1, 133–151, 2005.
2. Wu, P. H., "On sensitivity analysis of low probability of intercept (LPI) capability," *IEEE Conference on Military Communications*, 2889–2895, Atlantic City, USA, October 17–20, 2005.
3. Fancey, C. and C. M. Alabaster, "The metrication of low probability of intercept waveforms," *2010 International Conference on Waveform Diversity and Design*, 58–62, Niagara Falls, USA, August 8–13, 2010.
4. Deng, H., "Waveform design for MIMO radar with low probability of intercept (LPI) property," *2011 IEEE International Symposium on Antennas and Propagation (APSURSI)*, 305–308, Spokane, USA, July 3–8, 2011.
5. Schleher, D. C., "LPI radar: Fact or fiction," *IEEE Aerospace and Electronic Systems Magazine*, Vol. 21, No. 5, 3–6, 2006.
6. Stove, A. G., A. L. Hume, and C. J. Baker, "Low probability of intercept radar strategies," *IEE Proceedings — Radar, Sonar and Navigation*, Vol. 151, No. 5, 249–260, 2004.
7. Layne, J. R. and U. C. Piyasena. "Adaptive interacting multiple model tracking of maneuvering targets," *Proceedings of 16th Digital Avionics Systems Conference*, Vol. 1, 16–23, Ohio, USA, 1997.
8. Mazor, E., A. Averbuch, Y. Bar-Shalom, and J. Dayan, "Interacting multiple model methods in target tracking a survey," *IEEE Transactions on Aerospace and Electronic Systems*, Vol. 34, No. 1, 103–123, 1998.
9. Seah, C. E. and I. Hwang. "Algorithm for performance analysis of the IMM algorithm," *IEEE Transactions on Aerospace and Electronic Systems*, Vol. 47, No. 2, 1114–1124, 2011.
10. Gordon, N. J., D. J. Salmond, and A. F. M. Smith, "Novel approach to nonlinear/non-Gaussian Bayesian state estimation," *IEE Proceedings — Part F: Radar & Signal Processing*, Vol. 140, No. 2, 107–113, 1993.
11. Hong, S., L. Wang, Z.-G. Shi, and K. S. Chen, "Simplified particle phd filter for multiple-target tracking: Algorithm and architecture," *Progress In Electromagnetics Research*, Vol. 120, 481–498, 2011.
12. Wang, X., J.-F. Chen, Z.-G. Shi, and K. S. Chen, "Fuzzy-control-

- based particle filter for maneuvering target tracking,” *Progress In Electromagnetics Research*, Vol. 118, 1–15, 2011.
13. Yuan, L., Y. F. Zheng, J. Zhu, et al., “Object tracking with particle filtering in fluorescence microscopy images: Application to the motion of neurofilaments in axons,” *IEEE Transactions on Medical Imaging*, Vol. 31, No. 1, 117–130, 2012.
  14. Hong, L., N. Cui, M. Bakich, and J. R. Layne, “Multirate interacting multiple model particle filter for terrain-based ground target tracking,” *IEE Proceedings Control Theory & Applications*, Vol. 153, No. 6, 721–731, 2006.
  15. Boers, Y. and J. N. Driessen, “Interacting multiple model particle filter,” *IEE Proceedings Radar, Sonar and Navigation*, Vol. 150, No. 5, 344–349, 2003.
  16. Hong, S.-M. and Y.-H. Jung, “Optimal scheduling of track updates in phased array radars,” *IEEE Transactions on Aerospace and Electronic Systems*, Vol. 34, No. 3, 1016–1022, 1998.
  17. Lynch, Jr., D., *Introduction to RF Stealth*, Northwestern Polytechnical University Press, 2004.
  18. Clayton Kerce, J., G. C. Brown, and M. A. Mitchell, “Phase-only transmit beam broadening for improved radar search performance,” *IEEE Conference on Radar*, 451–456, 2007.